Chapter 3 Numerical Global Mode Shape Frequency Sensitivity Analysis

3.1. *Purpose*

The purpose of the GMSF sensitivity analysis on the FEM was in the first place to investigate the feasibility of damage quantification and qualification in a fan assembly by making use of the frequency shifts of global mode shapes. Secondly, it was used to identify certain GMSFs that may be useful in damage detection of the FaBCoM TeSt during testing.

The influences of several operational variables on GMSF shift were studied in order to identify GMSFs that are not only insensitive to these variables, but are also good indicators of damage location and extent. The variables used in the analysis included temperature, accumulated debris mass and rotational velocity. Different damage case scenarios in terms of number and position of cracked blades were also considered.

This analysis will be done by performing modal analyses on the FEM for each of the different variables and then comparing the obtained GMSFs for each set of results.

3.2. *Description*

For each operational condition variable, numerical modal analyses were performed on the FEM over a 2 kHz bandwidth for different levels of damage in the east blade (see Figure 3-1) at 0%, 25% and 50% damage. The damage level of an individual fan blade is defined in this dissertation as the percentage of blade root crack length of the total blade width.

3.2.1. Material Properties

Initially, the modal sensitivity analysis was performed for material properties obtained from Benham et al. [3] for carbon steel and aluminium alloy. These properties are listed in Table 3-1 for the FEM before and after model updating.

Table 3-1: Material Properties Used in FEM

Material Name	Pre/post Model Updating	Young's Modulus [GPa]	Density [kg.m^{-3}]	Temperature Expansion Coefficient [x10^{-6}.°C^{-1}]	Poisson's Ratio
Steel	Pre	208	7850	12	0.3
	Post	192.6	7756.3	12	0.3
Aluminium	Pre and Post	70	2710	23	0.33

It was discovered that the modal frequencies obtained from the FEM modal analysis were rather quite sensitive to material properties. For this reason, model updating was performed in terms of material property updating for all the FEM elements to which the steel properties were assigned. The specific material properties updated were Young's modulus and material density.

The procedure of experimentally determining these material properties is described in Chapter 4.

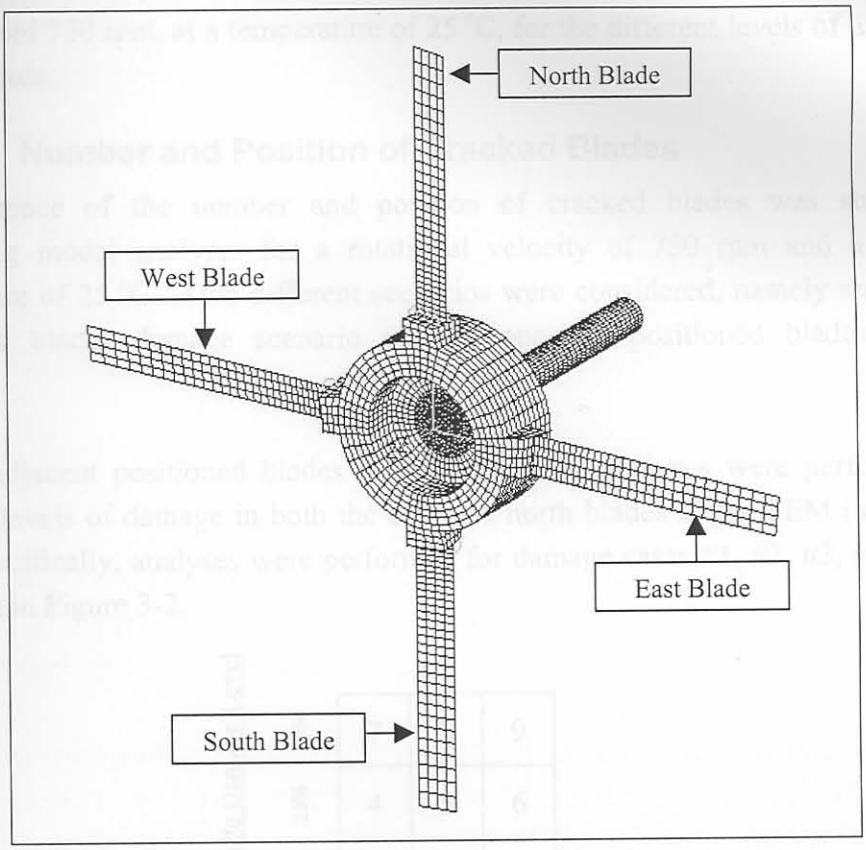

Figure 3-1: Blade Naming on FEM

3.2.2. Thermal Sensitivity

Thermal sensitivity was investigated by performing modal analyses for three different levels of temperature namely 25 °C, 50 °C and 75 °C at a rotational velocity of 750 rpm, for the different damage levels of the east blade.

3.2.3. Debris Mass Sensitivity

The purpose of this part of the analysis was to determine the effect of accumulated debris on modal frequencies. As a first approach, analyses were run for single point masses added to the leading tip of each blade. The masses used were 2.1 g, 4.2 g and 6.3 g, with 2.1 g being the mass of a typical accelerometer such as used in the EMA.

As obtained from Garnett-Bennett [19], debris mass accumulation on an actual fan found at Majuba Power Station is negligible at a maximum of 40 g spread over the lower third surface area of a fan blade, taking into account that the length of a single blade is over 0.7 m. However, this part of the analyses did prove useful as added point masses showed rather noticeable frequency shifts. This was taken into account when the experimental modal analysis was performed.

3.2.4. Rotational Velocity Sensitivity

This part of the analysis was performed for different rotational velocities of 150 rpm, 450 rpm and 750 rpm, at a temperature of 25 °C, for the different levels of damage of the east blade.

3.2.5. Number and Position of Cracked Blades

The influence of the number and position of cracked blades was studied by performing modal analyses for a rotational velocity of 750 rpm and a material temperature of 25 °C. Two different scenarios were considered, namely an adjacent positioned blades damage scenario and an opposite positioned blades damage scenario.

For the adjacent positioned blades damage scenario, analyses were performed for different levels of damage in both the east and north blades of the FEM (see Figure 3-1). Specifically, analyses were performed for damage cases #1, #2, #3, #5, #6 and #9 shown in Figure 3-2.

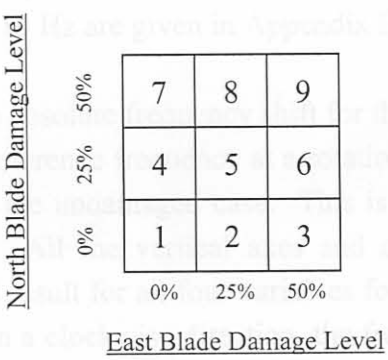

Figure 3-2: Adjacent Positioned Blades Damage Case Matrix

The reason why only these six damage cases are analysed, is that the assumption is made that the frequency shift result matrices are symmetric. In other words, the assumption is made that the analyses for damage cases #2, #3 and #6 will yield the same results as for damage cases #4, #7 and #8 respectively in terms of GMSFs.

For the opposite positioned blades damage scenario, analyses were performed for different levels of damage in the east as well as the west blade (see Figure 3-1). The same damage cases are considered as for the adjacent blade damage scenario, if Figure 3-2 is drawn for west blade damage level on the vertical axis.

3.3. Ideal Results

The ideal mode shape will be one of which the frequency shift is independent of operational variables such as rotational velocity and temperature but at the same time is a very good quantifier and qualifier of damage. This means that the GMSF should be sensitive to a specific damage scenario to allow for easy damage detection for that damage scenario. This in turn means that different GMSF should be identified for each damage scenario in order to detect damage for all damage scenarios.

3.4. Typical Results

It is not possible to identify fixed trends of the results in terms of sensitivity of mode shape order to damage. However, GMSFs above 240 Hz (global mode shapes #10 and up) are much more sensitive to the considered variables with maximum frequency shifts of 10 Hz and higher. Overall, GMSFs above 1200 Hz (global mode shapes #28 and up) tend to yield the best results in terms of damage sensitivity with a few exceptions being sensitive to rotational velocity and temperature.

The results obtained from the modal sensitivity analysis are graphically represented for four sensitivity parameters namely rotational velocity, temperature, adjacent positioned blades damage levels and opposite positioned blades damage levels in Figure 3-3 to Figure 3-6 for the 4^{th}, 5^{th}, 34^{th} and 35^{th} mode shapes respectively. The results for all the mode shapes within a 2 kHz bandwidth with a maximum absolute frequency shift of at least 10 Hz are given in Appendix B.

Each figure represents the absolute frequency shift for that mode shape relative to that particular mode shape's reference frequency at a rotational velocity of 750 rpm and a temperature of 25 ^{o}C for the undamaged case. This is given on the vertical axes as well as the colour bars. All the vertical axes and colour bars are scaled to the maximum frequency shift result for all four variables for each individual mode shape. From the top left, going in a clockwise direction, the frequency shift results are given for the rotational velocity, temperature, opposite positioned blades damage level and adjacent positioned blades damage level variables.

In Figure 3-3 the results for the 4^{th} mode shape with a reference frequency of about 35 Hz is given. The frequency of the 4^{th} mode shape is an example of a GMSF that is much more sensitive to rotational velocity than to the other variables. Other similar mode shapes within a bandwidth of 2000 Hz were found to be mode shapes #1, #2, #3, #6 to #9, #20, #21, #23, #24, #27 and #31. This implies that the frequencies of these mode shapes are more affected by rotational stiffening than damage.

In Figure 3-4, the results for the 5^{th} modal frequency at about 70 Hz, which is first torsional mode of the shaft, are shown. The reason for the temperature dependency of the mode shape is that the FEM boundary conditions, as discussed in Chapter 2, also constrain the shaft in the axial direction. In other words, the shaft is not allowed to expand in the axial direction as a result of temperature effects at the constrained nodes. This introduces axial stress of the shaft between the constrained nodes, affecting the stiffness of the shaft.

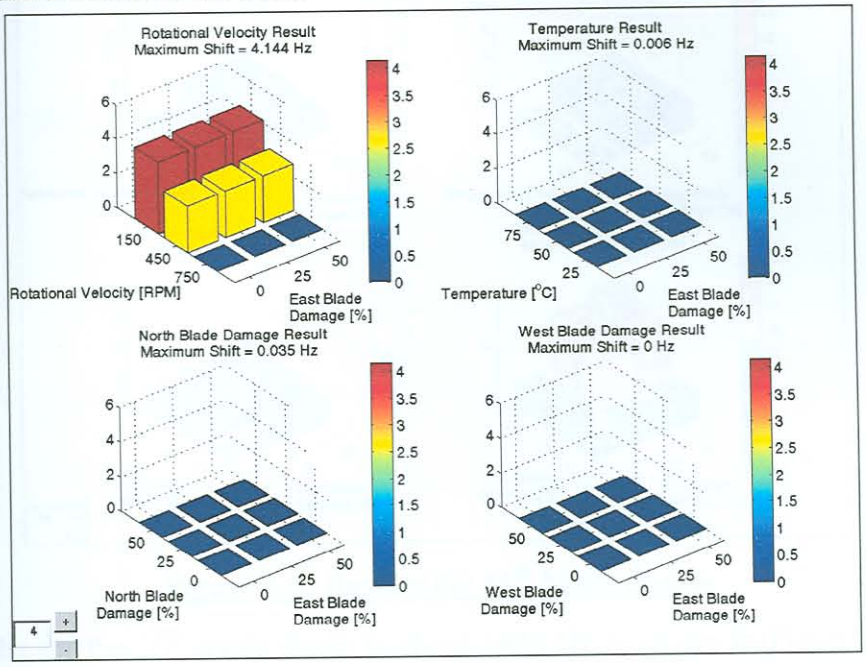

Figure 3-3: Results of 4th Mode Shape

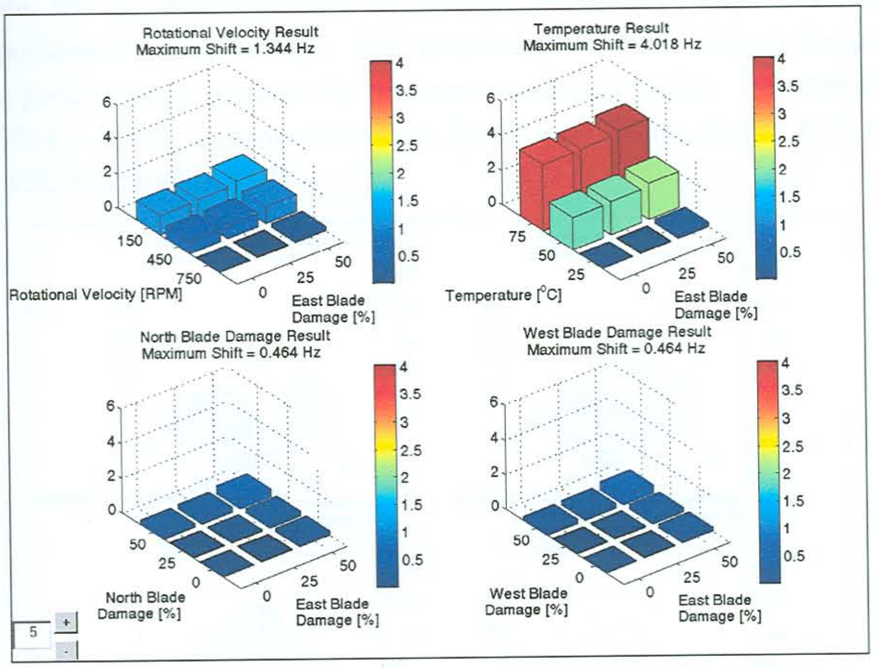

Figure 3-4: Results of 5th Mode Shape

Figure 3-5 shows the results for the 34th mode shape that has a reference frequency of about 1648 Hz. This mode shape is an example of a mode of which the frequency is relatively independent of rotational velocity and temperature, and is more dependant on damage levels for opposite positioned blades than adjacent positioned blades. This makes the frequency of this mode shape a good damage indicator for opposite positioned blades damage. Other similar mode shapes were found to be mode shapes #16, #21, #25, #29, #36 and #40 within a 2000 Hz bandwidth.

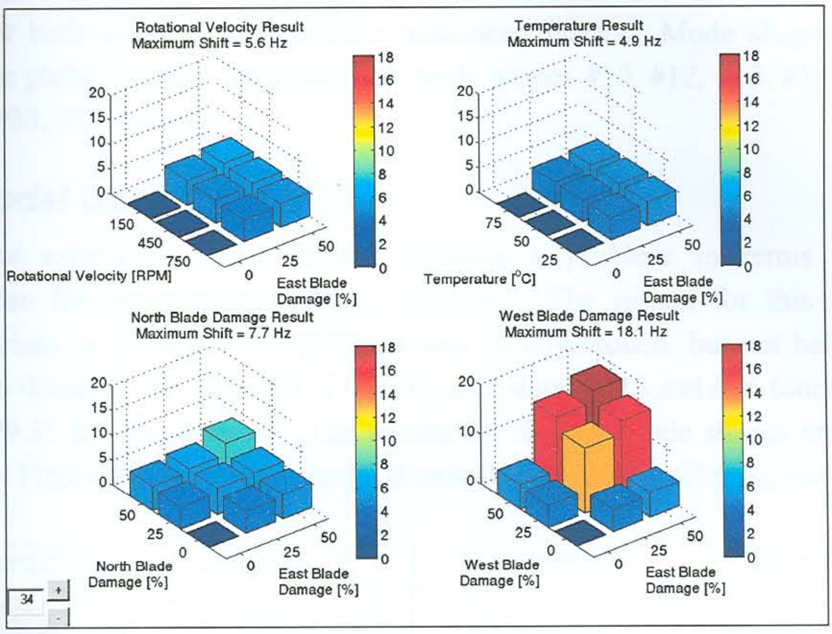

Figure 3-5: Results for 34th Mode Shape

The results for the 35th mode shape at about 1676 Hz is shown in Figure 3-6. This mode shape's frequency is again relatively independent of rotational velocity and temperature, and is more dependent on adjacent positioned blades damage than on opposite positioned blades damage. This means that the mode shape's frequency is in this case a good damage indicator for adjacent positioned blades. Other similar mode shapes within a 2000 Hz bandwidth were found to be mode shapes #11, #14, #18, #22, #26, #30, #37, #39 and #41.

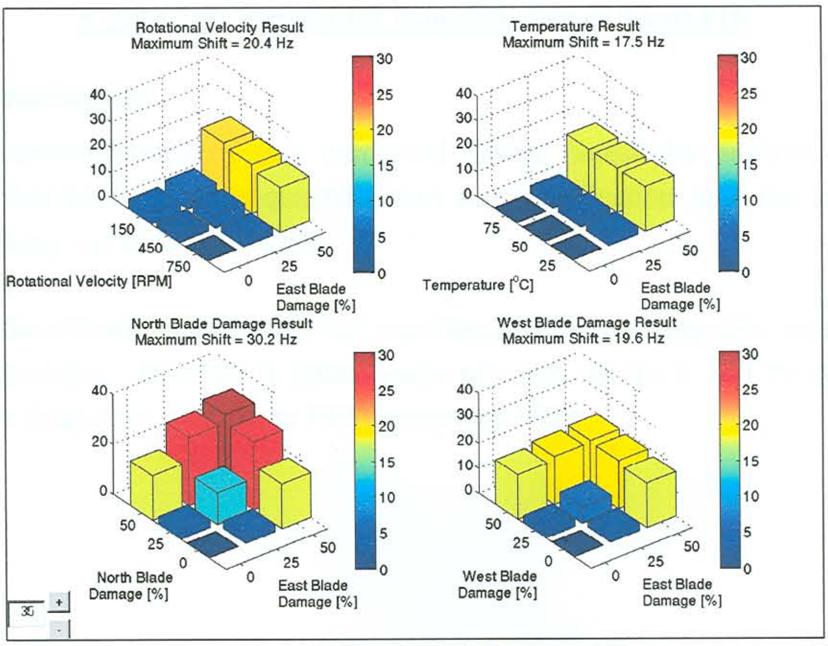

Figure 3-6: Results for 35th Mode Shape

Some mode shape frequencies were found to be good global structural damage indicators. In other words, these mode shapes' frequencies are again relatively independent of rotational velocity and temperature, and are dependent equally of damage for both adjacent and opposite positioned blades. Mode shapes that were found to be global damage indicators are mode shapes #10, #12, #13, #15, #17, #19, #28, #32, #33, #38 and #42.

3.5. Modal Density

As can be expected, modal density presents a problem in terms of GMSF identification for experimental testing purposes. The reason for this is that the situation arises of a number of GMSFs being closely spaced, but not being equally sensitive to damage. An example of this is mode shapes #15 and #16 found at 399.08 Hz and 399.35 Hz respectively. The results for the two mode shapes are shown in Figure 3-7. Figure 3-8 presents a modal density histogram for GMSFs using bin sizes of 10 Hz:

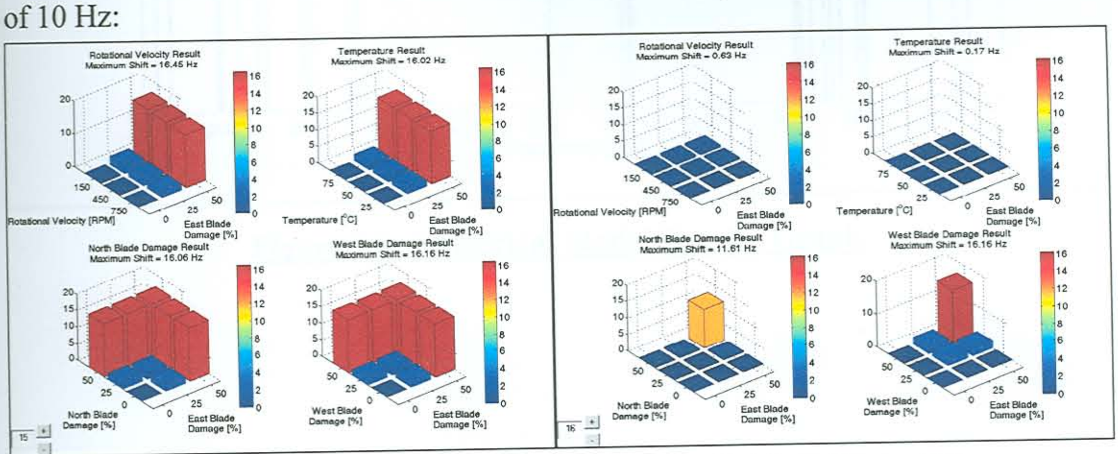

a) Mode Shape #15 *b) Mode Shape #16*

Figure 3-7: Results for Mode Shapes #15 and #16

3.6. Conclusion

From the results yielded by this numerical GMSF sensitivity analysis, it can be concluded that blade damage quantification and qualification of a fan assembly is feasible making use of GMSF shifts.

As to the identification of GMSFs for experimental testing purposes, modal density presents a problem. In order to obtain more relevant results, it will be necessary to look at peak frequency shifts from FEM generated FRFs.

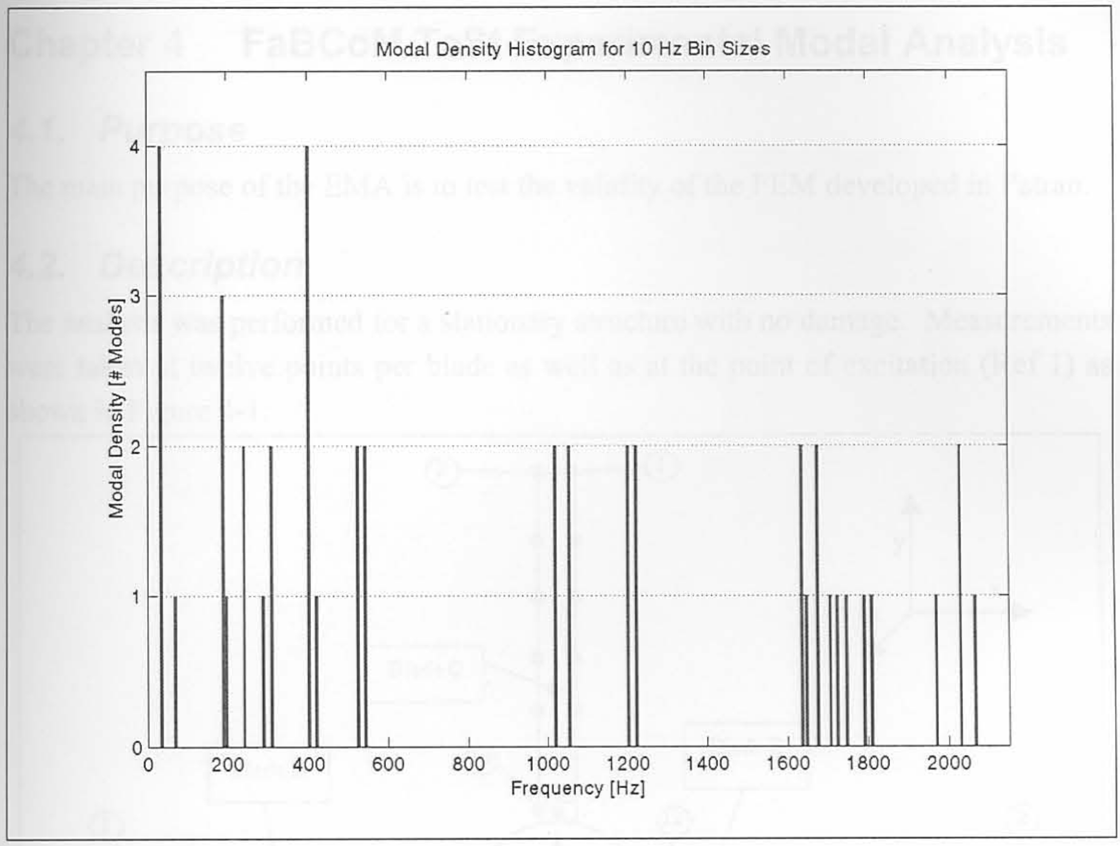

Figure 3-8: Numerical Modal Density Graph